Laser-assisted vibrational control of precursor molecules in diamond synthesis

Yun Shen Zhou, Li Sha Fan, Zhi Qiang Xie, Lan Jiang, Jean-François Silvain, Yong Feng Lu

Laser-Assisted Vibrational Control of Precursor Molecules in Diamond Synthesis

Yun Shen Zhou[1], Li Sha Fan[1], Zhi Qiang Xie[1], Lan Jiang[2], Jean-François Silvain[3], and Yong Feng Lu[1*]

[1]Department of Electrical Engineering, University of Nebraska-Lincoln, Lincoln, NE 68588-0511, USA

[2]School of Mechanical Engineering, Beijing Institute of Technology, Beijing 100081, China

[3]Institut de Chimie de la Matière Condensée de Bordeaux (ICMCB), CNRS, 33608 Pessac, France

***Corresponding Author:** Prof. Yong Feng Lu; Department of Electrical Engineering, University of Nebraska-Lincoln, Lincoln, NE 68588-0511, USA; Email: ylu2@unl.edu; Tel.: 1-402-472-8323; Fax: 1-402-472-4732.

Abstract: Control of chemical reactions is the essence of chemistry, producing designed outcomes while suppressing unwanted side products. Laser-assisted molecular vibrational control has been demonstrated to be a potential approach to influencing the outcome of a chemical reaction. In this article, we reviewed recent progress in the laser control of diamond synthesis through vibrational excitation of precursor molecules in a laser-assisted combustion chemical vapor deposition process. Significantly promoted diamond deposition rate (139 μm/h) and crystalline quality were achieved by resonantly exciting the Q-branch ($\Delta J = 0$) of the CH_2-wagging mode (ν_7 mode 949.3 cm^{-1}) of C_2H_4 molecules. Resonant excitation of the fundamental vibration is more effective in promoting diamond growth than vibrational excitation. Control of diamond crystallographic orientation was also realized by resonantly exciting the R branch ($\Delta J = 1$) of the CH_2-wagging mode of C_2H_4 molecules and resulted in the preferential growth of {100}-oriented diamond crystals. Nitrogen-doped diamond films with a nitrogen concentration of 1.5×10^{20} atoms/cm^3 were synthesized by resonantly exciting the rotational-vibrational transition ($J=5 \rightarrow J'=6$, $K=0$) of the N-H wagging mode (ν_2 mode) in ammonia molecules. The findings demonstrate the feasibility of laser-assisted vibration control in steering chemical reactions and controlling reaction outcomes.

Keywords: Diamond; thin film; vibrational excitation; laser; combustion chemical vapor deposition.

Introduction

The essence of chemistry is achieving precise control of chemical reactions towards anticipated outcomes while suppressing unwanted side products [1-6]. Conventionally, chemical reactions can be influenced either dynamically, varying external parameters such as temperature, pressure, and concentration, or kinetically, such as utilizing catalysts [1-6]. Since the invention of lasers, laser intervention has been a conceptually appealing tactic to steering chemical reactions and influencing final outcomes. Laser-matter interactions can be either a thermal process or a non-thermal process [1-6]. For a thermal process, incident photons are used primarily as a heating source, in which laser energy is generally deposited into specific reactants and dispersed rapidly to other molecules achieving an equilibrium thermal heating. Similar to conventional thermal driven chemical reactions, the laser thermal process is short of reaction selectivity [1-6]. For a non-thermal process, laser control of chemical reactions can be realized via a number of mechanisms, including 1) controlling molecular vibrational states; 2) photo-isomerization of reactant molecules; 3) exciting electrons to states of different bonding properties; and 4) regulating electron populations at different states [1-6].

Laser-assisted vibrational excitation of molecules is an intuitively attractive approach realizing laser control of chemical reactions [1-6]. In 1972, Polanyi introduced the concept of mode-selective chemistry [7-10], in which vibrational excitation along the reaction coordinate would be more effective than translational motion in promoting endoergic reactions, e.g. the mode of internal excitation could control the reaction outcome. It is expected that the excitation of fundamental vibration or overtone vibration of higher levels would selectively localize energy in a specific bond or a motion along the reaction coordinate, lead to the preferential cleavage of the corresponding bond, and achieve reaction pathway control [7-10]. Extensive investigation on simple molecules, such as HOD [11] (an isotopic variant of water), HCN + Cl [12], and ND_3 + NH_3 [13], has confirmed the validity of the conjecture. Crim reported selective cleavage of chemical bonds and achieving chemical reaction control via vibrational excitation [2,11,12,14], In the reaction of CH_3D with Cl, excitation of the first overtone of C-D stretch ($2\nu_2$) mode leads to the selective cleavage of the C-D bonds and produces CH_3 exclusively [14]. While the excitation of the C-H stretch (symmetric ν_1 and antisymmetric ν_4) results in the selective cleavage of C-H bonds and produce CH_2D only [14]. Grucebele reported that molecular vibrational energy is of fundamental importance in initiating polyatomic molecule reactions [15]. Keuster revealed that an infrared laser could energize ethylene molecules selectively to highly excited states and differentiate the energy transfer rates from resonant modes to a chemical exit channel [16-18]. However current investigation on the vibrationally controlled chemistry is still limited to small molecules. Extending the lab-bench concept to more complex reactants and field-scale material synthesis is still a challenge.

Due to its wide range of the most and best properties, diamond has been applied in a wide range of applications. In recent years, we investigated the laser-assisted vibration control of diamond synthesis through vibrational excitation of precursor molecules in a laser-assisted combustion chemical vapor deposition (LA-CCVD) process [19-23]. Significantly promoted diamond deposition rate (139 μm/h) and crystalline quality were achieved by resonantly exciting the Q-branch ($\Delta J = 0$) of the CH_2-wagging mode (a type *c* fundamental band, ν_7, at 949.3 cm^{-1}) of ethylene (C_2H_4) molecules [19,20]. Resonant excitation of the fundamental vibration (CH_2-wagging mode, ν_7) is more effective in laser energy coupling and promoting diamond deposition than vibrational excitation [22]. Control of diamond crystallographic orientation was realized by resonantly exciting the R branch ($\Delta J = 1$) of the CH_2-wagging mode of C_2H_4 molecules and resulted in the preferential growth of {100}-oriented diamond crystals [23]. Nitrogen-doped diamond films with a nitrogen concentration of 1.5 × 10^{20} atoms/cm^3 were synthesized by resonantly exciting the rotational-vibrational transition (J=5 → J'=6, K=0) of the N-H wagging mode (ν_2 mode) in ammonia molecules [21]. The findings

demonstrate the feasibility of converting the lab-bench concept to practical material synthesis.

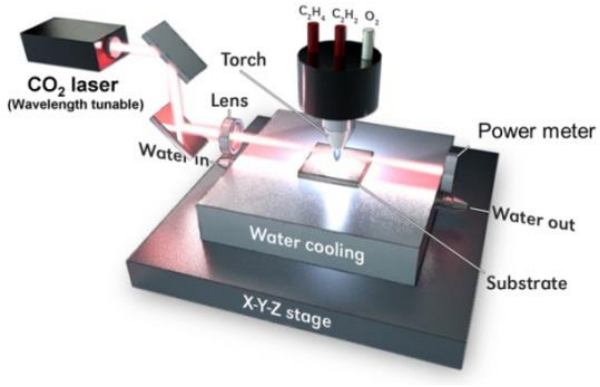

Figure 1. A schematic experimental setup of the LA-CCVD system.

A LA-CCVD system, as shown in Fig. 1, was deployed for growing diamond in open air by using acetylene (C_2H_2), ethylene (C_2H_4), and oxygen (O_2) as precursors. A wavelength tunable (9.2 to 10.9 μm) continuous wave (CW) CO_2 laser was used as the irradiation source to intervene the diamond growth process [19-23].

Based on the first law of photochemistry, the Grotthuss-Draper law, the incident light must be absorbed by a reactant in order to initiate a reaction. Since acetylene does not show obvious absorption peaks within the CO_2 laser wavelength range (9.2 to 10.9 μm), ethylene is added into the oxy-acetylene flames due to its obvious absorption bands within the wavelength range, as shown in Fig. 2a. Among several absorption peaks observed, two strongest peaks at 10.532 and 10.22 μm are chosen for investigating vibration control of diamond synthesis [19,20,22,23]. The strongest absorption peak at 10.532 μm is ascribed to the Q branch ($\Delta J = 0$) of the CH_2-wagging mode (a type *c* fundamental band, ν_7, at 949.3 cm^{-1}, equivalent to a wavelength of 10.534 μm) of ethylene molecules, as shown in Fig. 2b, involving vibrational excitation only. While the second strongest absorption peak at 10.22 μm is attributed to the R branch ($\Delta J = 1$) of the CH_2-wagging mode of ethylene molecules, as shown in Fig. 2b, involving both vibrational and rotational excitation. Selective excitation of individual vibration controls competition among diamond formation pathways and leads to different outcomes [19,20,22,23].

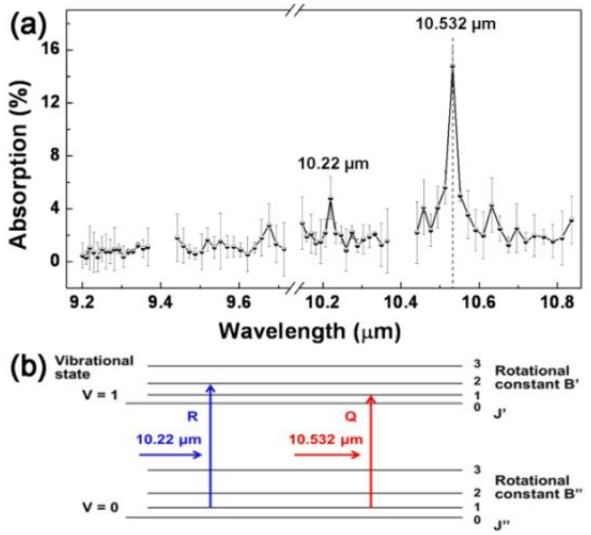

Figure 2. (a) A typical absorption spectrum of the $C_2H_2/C_2H_4/O_2$ flames as a function of laser wavelength from 9.2 to 10.9 μm. (b) Vibration-rotation transitions of an ethylene molecule at 10.22 and 10.532 μm, respectively.

Selectively Promoted Diamond Growth by Vibrational Excitation of Ethylene Molecules

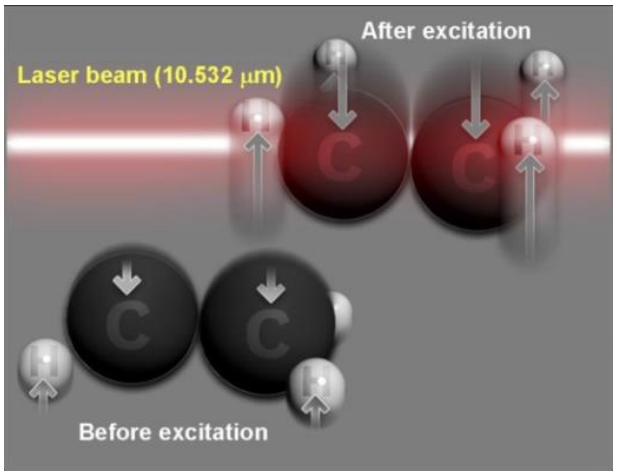

Figure 3. A schematic of the resonantly excited CH_2-wagging mode (a type *c* fundamental mode, ν_7) of an ethylene molecule.

Among 12 vibrational modes of ethylene molecules, the butterfly-like CH_2-wagging mode (949.3 cm^{-1} or 10.534 μm), Fig. 3, demonstrates a

strong infrared activity and matches closely with the 10.532 μm emission line of the CO_2 laser. Selective excitation of the CH_2-wagging mode could lead to exciting ethylene molecules from the ground state to the first level of excited vibrational state and result in effective energy coupling into the reactants. The influence of the coupled laser energy can be twofold, 1) dispersed as thermal energy and increasing the overall temperature and 2) selectively activating specific species above a particular energy barrier towards corresponding reaction channels. However, it should be pointed out that resonant excitation of the CH_2-wagging mode alone cannot lead to the direct bond breaking of the C-H bonds in ethylene molecule due to insufficient incident laser power density. Further high-level excitation and dissociation of ethylene molecules are ascribed to the energy pooling effect due to molecular collisions. To verify the influence and selectivity of the vibrational excitation in reaction control, the diamond growth process using acetylene-ethylene-oxygen flames was investigated by tuning laser parameters, including wavelength and output power density.

Due to the wavelength-dependent absorption rate, the wavelength of the incident laser can significantly impact the shape and temperature of the acetylene-ethylene-oxygen flames as shown in Fig. 4, in which the fundamental v_7 mode and neighboring vibrational modes are excited. When resonantly exciting the fundamental v_7 mode at 10.532 μm, the flame reaches the maximum laser energy absorption rate, highest temperature and shortest flame length, as shown in Fig. 4a to 4c, indicating effective energy coupling and stimulated reactions. The increased flame temperature can stimulate the formation of atomic hydrogen, which helps improving diamond phase purity by etching away non-diamond carbons. The vibrational excitation obviously influences the concentrations of reactive species in the flames, including C_2, CH and OH, as shown in Fig. 4d. It is generally accepted that C_2 is a beneficiary species stimulating the diamond growth [24],

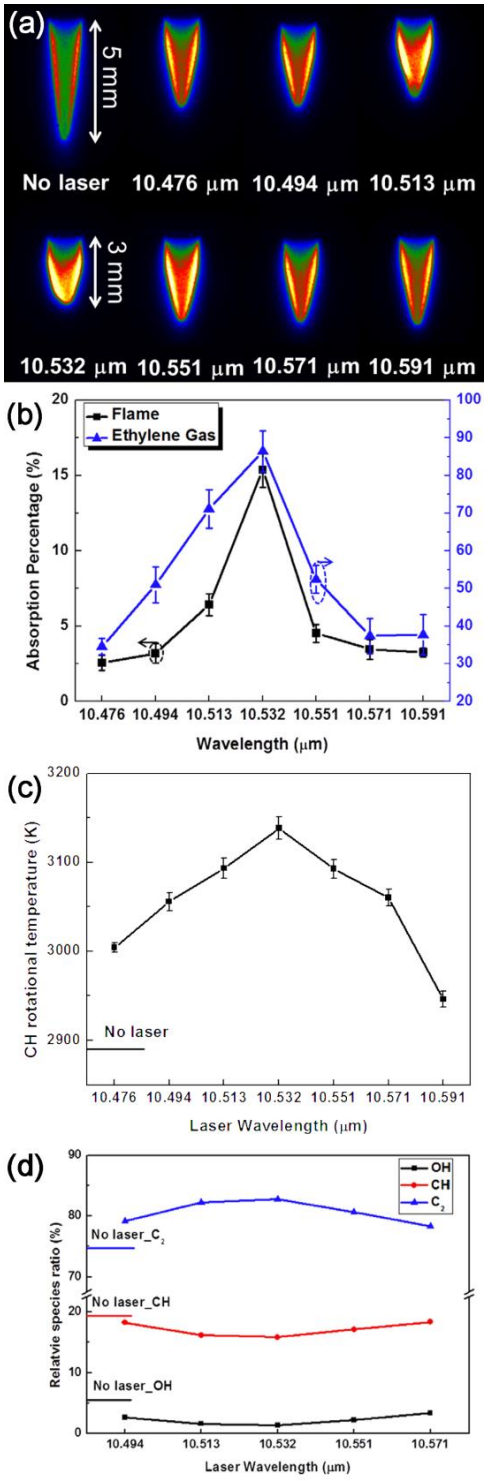

Figure 4. Influence of the laser wavelength: (a) optical images of the acetylene-ethylene-oxygen flames; (b) laser energy absorption rates of the flame (left) and ethylene gas (right); (c) flame temperature; and (d) relative species ratios as the functions of the laser wavelength.

while OH is a carbon etchant [25]. The resonant excitation of the fundamental v_7 mode effectively raises the concentration of C_2, suppresses that of CH and OH, and leads to the selectively promoted diamond growth, as shown in Fig. 5 and 6. Diamond particle size, crystalline quality, and deposition rate are significantly improved by introducing vibration excitation and reach the highest values when resonantly exciting the v_7 mode [22].

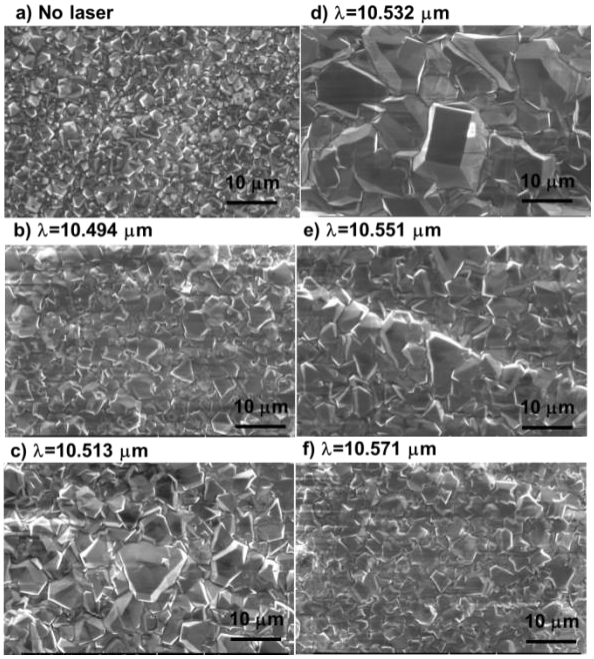

Figure 5. Influence of the laser wavelength: SEM micrographs of diamond films deposited using the LA-CCVD method without laser irradiation and with laser irradiation at different wavelengths.

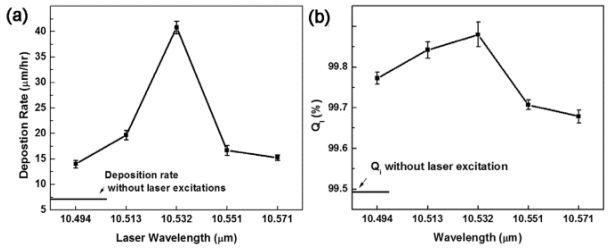

Figure 6. Influence of the laser wavelength: (a) diamond deposition rate and (b) diamond quality factor (Q) as a function of laser wavelength.

Laser power density also plays a critical role in influencing the growth of diamond [19]. As shown in Fig. 7a, the flame length decreases consistently with a broadened width as the laser power density increases, indicating the accelerated reactions. The brightness of the flame also increases continuously as the laser power density rises, representing a higher flame temperature and accelerated reactions. Although the absorbed laser power increases continuously with the rising laser power density, the absorption coefficient decreases due to the saturated laser power absorption. The absorption saturation is ascribed to the anharmonic shift between high-laying vibrational states and decreased absorption cross-sections [26].

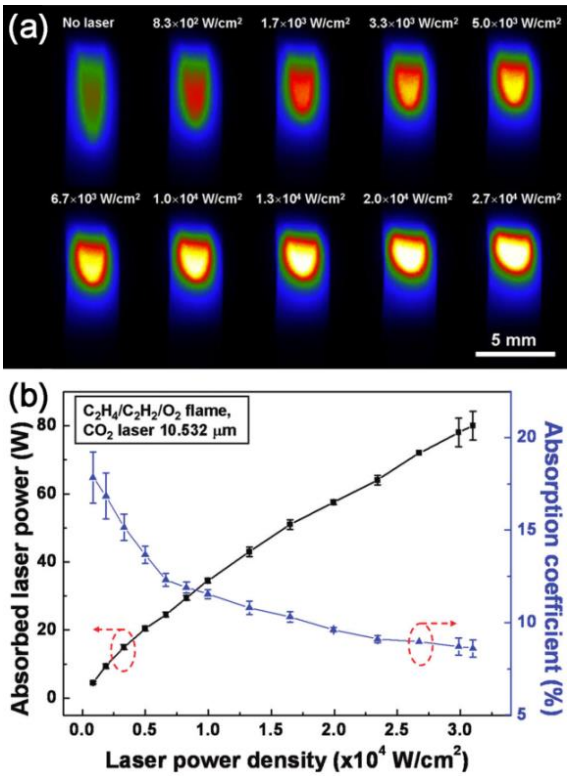

Figure 7. Influence of the laser power density: (a) optical images of the acetylene-ethylene-oxygen flames without laser irradiation and with laser irradiation at different laser power densities, and (b) absorber laser power (left) and absorption coefficient (right) with respect to incident laser power densities, laser wavelength: 10.532 μm.

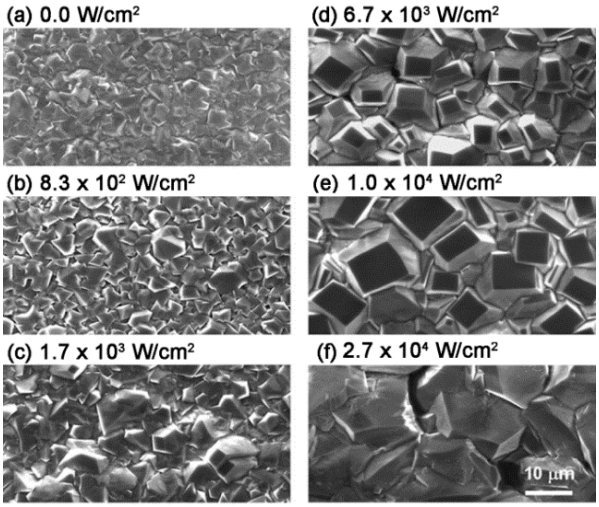

Figure 8. Influence of the laser power density: SEM micrographs diamond films deposited using the LA-CCVD method with laser irradiation at different power densities.

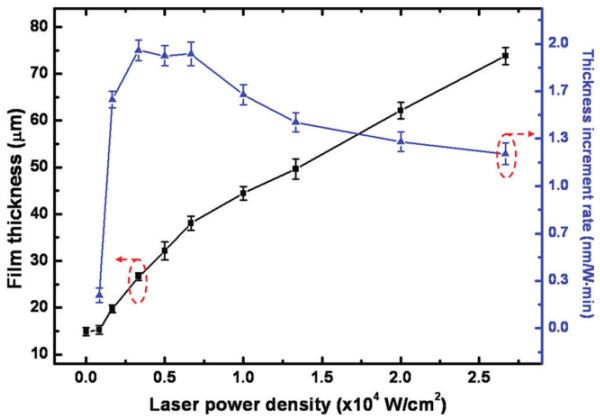

Figure 9. Influence of the laser power density: diamond film thickness (left) and deposition rate (right) as the functions of laser power density.

As the results of the laser power absorption saturation, controlling the incident laser power density can significantly influence the diamond growth in terms of crystalline morphology, grain size, deposition rate, and quality, as shown in Fig. 8 and 9 [19]. When the laser power density increases, diamond grain size increases constantly. Diamond films consisting of dominantly {100} oriented diamond crystals are deposited within a narrow power density window, between 5.0×10^3 and 1.0×10^4 W/cm^2. Otherwise, randomly oriented diamond grains are obtained. The random-(100)-random morphology change is ascribed to the increased C_2 concentration in the flames when the laser power density rises. As reported, adding C_2 into C-H bonds of H-terminated diamond (100) surfaces is energetically favorable on monohydride surfaces [27,28]. Therefore, continuous diamond growth can readily start from existing diamond crystals and the (100) facet crystals will dominate. However, when the laser power density surpasses a critical point, 1.0×10^4 W/cm^2 in our studies, over abundant C_2 radicals leads to unhydrided surfaces and results in secondary nucleation from existing crystals, therefore ruining the crystalline orientation selectivity. Although the diamond film thickness increases constantly as the laser power density rises, the thickness increment rate (nm/W-min) reaches its peak value between 3.3×10^3 and 6.7×10^3 W/cm^2 and starts to decrease gradually, indicating the saturated absorption, which coincides with the results in Fig. 7. Therefore, the highest laser energy efficiency the best quality diamond are achieved with a power density range between 5.0×10^3 and 6.7×10^3 W/cm^2.

Therefore, laser wavelength and power density are demonstrated playing critical roles in selectively controlling the diamond growth [19,20,22]. Selectively exciting the Q branch of the CH_2-wagging mode in ethylene molecules significantly promotes the growth rate and crystalline quality of diamond [19,20,22]. A growth rate of 139 μm/h was achieved with obviously improved sp^3 carbon phase purity.[20] Resonant vibrational excitation is demonstrated to be more effective than vibrational excitation in coupling incident laser energy and promoting the diamond growth [22]. For a fixed reactant material volume, incident laser power density also shows obvious influence in diamond growth rate and quality [19].

Crystallographic Orientation Control in Diamond Growth

Energy coupling via vibration excitation influences not only diamond growth rate and crystalline quality but also crystallographic orientation. By intervening different vibrational modes, laser energy is coupled into different channels achieving divergent outcomes.

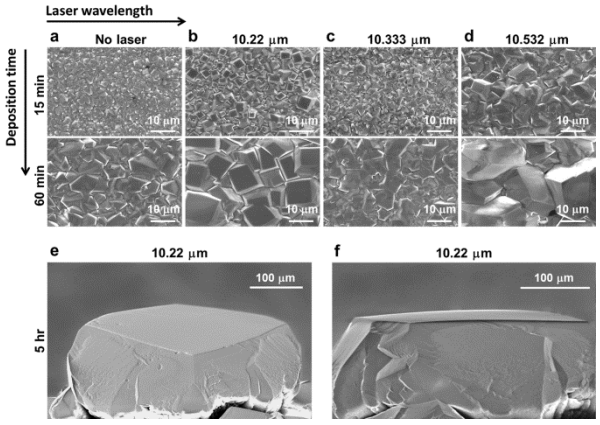

Figure 10. SEM micrographs of the diamond films and particles. (a-d) diamond films deposited without laser (a), with laser irradiation at 10.22 μm (b), 10.333 μm (c), and 10.532 (d). (e) and (f) single-crystal diamond grown with laser irradiation at 10.22 μm.

In this study, the R branch (ΔJ = 1) of the CH_2-wagging mode at 10.22 μm was resonantly excited, by which the ethylene molecules are excited to an excited vibrational state level with a higher rotational level, as schematically indicated in Fig. 2b [23]. Compared with diamond films deposited under other conditions, 10.22 μm irradiation results in the preferential growth of {100} textured diamond films, as shown in Fig. 10.

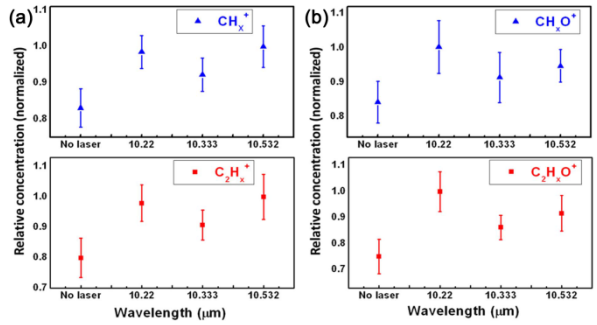

Figure 11. Mass spectrometry of $C_2H_2/C_2H_4/O_2$ flames. Relative concentrations of (a) C_xH_y (x = 1 and 2, y = 0 ~ 5) and (b) C_xH_yO (x = 1 and 2, y = 1 ~ 5) ions.

According to mass spectrometric studies, the preferential growth of the {100} textured diamond films is ascribed to the increased C_xH_yO ions as compared with flames irradiated at other wavelengths, such as 10.532 μm. As mentioned above, the 10.22 μm excitation pump ethylene molecules to a higher vibrational and rotational levels as shown in Fig. 2b. Since the rotational-translational translation is much faster than the vibrational-rotational translation for energy transfer, a higher rotational level will result in a more effective translational energy transition, therefore a higher flame temperature [23]. An increased flame temperature leads to a higher concentration of the C_xH_yO ions, which is also verified by Quantum Molecular Dynamics (QMD) simulations. Periodic Density-Functional Theory (DFT) simulations also demonstrate a higher reactivity on C{111} surfaces than C{100} surfaces, therefore a higher growth rate at the <111> direction, resulting in the preferential growth of {100} textured diamond films [23].

Synthesis of Nitrogen-Doped Diamond Films

The same vibrational excitation concept was also extended to other materials, such as nitrogen-doped diamond [21].

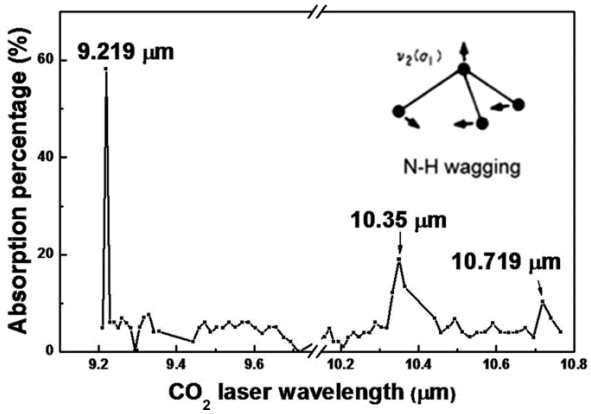

Figure 12. Absorption spectrum of the CO_2 laser power by NH_3 gas as a function of wavelength.

Doping diamond with nitrogen (N) can improve the electrical conductivity of the diamond [29]. However, a high dose of N addition easily leads to diamond structure and phase degradation [30]. Therefore, it is desired to realize effective N addition and still maintain satisfactory crystal quality. In this study, a NH_3 added oxy-acetylene flame is used for growing the N-doped diamond.

Figure 12 shows the absorption spectrum of gaseous NH_3 within a spectral range from 9.2 to 10.9 μm. Three prominent absorption peaks are observed at 9.219, 10.35 and 10.719 μm. The infrared absorption is ascribed to the v_2 N-H wagging mode of NH_3 molecules, which vibrates in an umbrella inversion mode [31]. Due to the barrier that the N encounted when traveling through the proton plane, the v_2 mode is split into two components at 932.51 (v_2+) and 968.32 (v_2-) cm^{-1}, respectively [31]. The 9.219 absorption peak arises from the rotational-vibrational transition aat 1084.63 cm^{-1} [5(J) to 6(J'), K = 0] in the v_2- band, which perfectly matches the laser line at 1084.71 cm^{-1} therefore results in a strong laser energy absorption and resonant excitation. Two peaks at 10.35 and 10.719 μm are ascribed to the Q-branch at 965.99 cm^{-1} [J = K = 5] in the v_2- mode and Q-branch at 932.40 cm^{-1} [J = K = 2] in the v_2+ mode, respectively [31]. The 0.5 cm^{-1} mismatch degrades the laser absorption rate at 10.35 and 10.719 μm.

Figure 13 shows SEM micrographs of the films deposited using the NH_3 added oxy-acetylene flame. As expected, cauliflower-like carbon balls consisting of sp^2 and sp^3 carbons are obtained without vibration excitaiton, as shown in Fig. 13b and 13c. With vibration excitation, diamond crystals start to appear, Fig. 13d and 13e. When resonantly excited at 9.219 μm, (111) faceted diamond particles are obtained with a N doping concentration of 1.5×10^{20} atoms/cm^3 [21], which is impossible by using conventional methods. The selective growth of N-doped diamond under vibrational excitation is ascribed to the concentrations of N-containing species in the flames. Vibrational excitation increases the concentrations of CNO and H_2CN, but supresses the concentratin of CN. The role of CN can be two-fold [32]. At a low concentration, CN ions derive H atoms from diamond surface, forming HCN/H_2CN and exposing diamond for continous growth. From the other aspect, CN ions tends to form cyanogen (**C_2N_2**), which leads to the formation of the cauliflower structures [32]. Therefore, selective growth of the N-doped diamond can be achieved by controlling the concentrations of the N-containing species by vibrational exctitation.

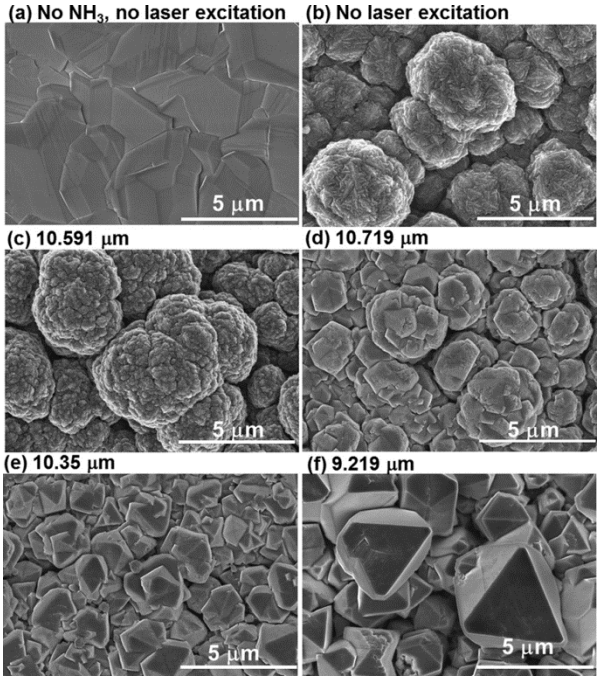

Figure 13. SEM micrographs of diamond films deposited using (a) NH_3-free flame without laser excitation, (b) NH_3-added flame without laser excitation, and (c - f) NH_3-added flame with laser excitation at 10.591, 10.719, 10.35 and 9.219 μm, respectively.

Conclusion

In conclusion, we investigated laser-assisted vibration control of diamond synthesis. Laser irradiation of matching wavelength was used to intervene the diamond growth process through vibrational excitation of precursor molecules. It is found that vibrational excitation of different states significantly influences the reaction processes and leads to different reaction outcomes. Selectively exciting the Q-branch ($\Delta J = 0$) of the CH_2-wagging mode of C_2H_4 molecules results in significantly promoted diamond deposition rate (139 μm/h) and crystalline quality. Resonant excitation of the fundamental vibration (CH_2-wagging mode, v_7) is more effective in laser energy coupling and promoting diamond deposition than vibrational excitation. Preferential growth of {100}-oriented diamond crystals is achieved by resonantly exciting the R branch ($\Delta J = 1$) of the CH_2-wagging mode of C_2H_4 molecules. Resonant excitation of the N-H wagging mode (v_2 mode) in NH_3

molecules effectively increases nitrogen concentration in Nitrogen-doped diamond. The results demonstrate the feasibility of laser-assisted vibration control of material synthesis for controllable and selective material synthesis.

Acknowledgement

The research work was financially supported by the U.S. Office of Naval Research (N00014-05-1-0432, N00014-09-1-0943, and N00014-09-7581-0943) and National Science Foundation (CMMI 1129613 and 1068510). The authors are grateful to Dr. I. Perez from the U.S. Office of Naval Research for his invaluable scientific advice and support.

References

1. Brumer P, Shapiro M: Laser control of chemical-reactions. Sci Am (1995) 272(3):56-&.
2. Crim FF: Chemical dynamics of vibrationally excited molecules: Controlling reactions in gases and on surfaces. P Natl Acad Sci USA (2008) 105(35):12654-12661.
3. Henriksen NE: Laser control of chemical reactions. Chem Soc Rev (2002) 31(1):37-42.
4. Quack M, Engel V, Manz J, Shapiro M, Woste L, Korolkov MV, Paramonov GK, Kellman ME, Child MS, Kobayashi T, Jain SR et al: General discussion on laser control of chemical reactions. Adv Chem Phys (1997) 101:373-388.
5. Torralva BR, Allen RE: Mechanisms for laser control of chemical reactions. J Mod Optic (2002) 49(3-4):593-625.
6. Zare RN: Laser control of chemical reactions. Science (1998) 279(5358):1875-1879.
7. Polanyi JC: Some concepts in reaction dynamics. Accounts Chem Res (1972) 5(5):161-&.
8. Polanyi JC: Some concepts in reaction dynamics - (nobel lecture). Angew Chem Int Edit (1987) 26(10):952-971.
9. Polanyi JC: Some concepts in reaction dynamics. Chem Scripta (1987) 27(2):229-247.
10. Polanyi JC: Some concepts in reaction dynamics. Science (1987) 236(4802):680-690.
11. Metz RB, Thoemke JD, Pfeiffer JM, Crim FF: Selectively breaking either bond in the bimolecular reaction of hod with hydrogen-atoms. J Chem Phys (1993) 99(3):1744-1751.
12. Metz RB, Pfeiffer JM, Thoemke JD, Crim FF: The reaction of chlorine atoms with highly vibrationally excited hcn. Chem Phys Lett (1994) 221(5-6):347-352.
13. Guettler RD, Jones GC, Posey LA, Zare RN: Partial control of an ion-molecule reaction by selection of the internal motion of the polyatomic reagent ion. Science (1994) 266(5183):259-261.
14. Yoon S, Holiday RJ, Crim FF: Vibrationally controlled chemistry: Mode- and bond-selected reaction of ch3d with ci. J Phys Chem B (2005) 109(17):8388-8392.
15. Gruebele M, Wolynes PG: Vibrational energy flow and chemical reactions. Accounts Chem Res (2004) 37(4):261-267.
16. Dekeuster D, Hemptinne XD: Physical and chemical relaxations in ethylene following co2-laser irradiation - time of flight observations. B Soc Chim Belg (1979) 88(1-2):1-12.
17. Dekeuster D, Hemptinne XD: Chemical relaxation in cw co2-laser irradiated ethylene at low-pressure. J Chem Phys (1979) 70(11):5319-5321.
18. Hemptinne XD: Contribution to photochemistry, ethylene laser. J Chim Phys Pcb (1979) 76(7-8):731-731.
19. Xe ZQ, He XN, Hu W, Guillemet T, Park JB, Zhou YS, Bai J, Gao Y, Zeng XC, Jiang L, Lu YF: Excitations of precursor molecules by different laser powers in laser-assisted growth of diamond films. Cryst Growth Des (2010) 10(11):4928-4933.
20. Xie ZQ, Zhou YS, He XN, Gao Y, Park J, Ling H, Jiang L, Lu YF: Fast growth of diamond crystals in open air by combustion synthesis with resonant laser energy coupling. Cryst Growth Des (2010) 10(4):1762-1766.
21. Fan LS, Xie ZQ, Park JB, He XN, Zhou YS, Jiang L, Lu YF: Synthesis of nitrogen-doped diamond films using vibrational excitation of ammonia molecules in laser-assisted combustion flames. J Laser Appl (2012) 24(2):022001.
22. Fan LS, Zhou YS, Wang MX, Gao Y, Liu L, F. SJ, Lu YF: Resonant vibrational excitation of ethylene molecules in laser-assisted diamond deposition. Laser Physics Letters (2014) 11:076002.
23. Xie ZQ, Bai J, Zhou YS, Gao Y, Park J, Guillemet T, Jiang L, Zeng XC, Lu YF: Control of crystallographic orientation in diamond synthesis through laser resonant vibrational excitation of precursor molecules. Sci Rep-Uk (2014) 4:4581.
24. Matsui Y, Yuuki A, Sahara M, Hirose Y: Flame structure and diamond growth-mechanism of acetylene torch. Jpn J Appl Phys 1 (1989) 28(9):1718-1724.
25. Komaki K, Yanagisawa M, Yamamoto I, Hirose Y: Synthesis of diamond in combustion flame under low-pressures. Jpn J Appl Phys 1 (1993) 32(4):1814-1817.
26. Yao L, Mebel AM, Lu HF, Neusser HJ, Lin SH: Anharmonic effect on unimolecular

reactions with application to the photodissociation of ethylene. J Phys Chem A (2007) 111(29):6722-6729.
27. Gruen DM, Redfern PC, Horner DA, Zapol P, Curtiss LA: Theoretical studies on nanocrystalline diamond: Nucleation by dicarbon and electronic structure of planar defects. J Phys Chem B (1999) 103(26):5459-5467.
28. Redfern PC, Horner DA, Curtiss LA, Gruen DM: Theoretical studies of growth of diamond (110) from dicarbon. J Phys Chem-Us (1996) 100(28):11654-11663.
29. Okano K, Koizumi S, Silva SRP, Amaratunga GAJ: Low-threshold cold cathodes made of nitrogen-doped chemical-vapour-deposited diamond. Nature (1996) 381(6578):140-141.
30. Atakan B, Beuger M, Kohse-Hoinghaus K: Nitrogen compounds and their influence on diamond deposition in flames. Phys Chem Chem Phys (1999) 1(4):705-708.
31. David CW: Ir vibration-rotation spectra of the ammonia molecule. J Chem Educ (1996) 73(1):46-50.
32. Hong TM, Chen SH, Chiou YS, Chen CF: Optical-emission spectroscopy studies of the effects of nitrogen addition on diamond synthesis in a ch4-co2 gas-mixture. Appl Phys Lett (1995) 67(15):2149-2151.

Figure captions

Figure 1. A schematic experimental setup of the LA-CCVD system.

Figure 2. (a) A typical absorption spectrum of the $C_2H_2/C_2H_4/O_2$ flames as a function of laser wavelength from 9.2 to 10.9 μm. (b) Vibration-rotation transitions of an ethylene molecule at 10.22 and 10.532 μm, respectively.

Figure 3. A schematic of the resonantly excited CH_2-wagging mode (a type *c* fundamental mode, v_7) of an ethylene molecule.

Figure 4. Influence of the laser wavelength: (a) optical images of the acetylene-ethylene-oxygen flames; (b) laser energy absorption rates of the flame (left) and ethylene gas (right); (c) flame temperature; and (d) relative species ratios as the functions of the laser wavelength.

Figure 5. Influence of the laser wavelength: SEM micrographs of diamond films deposited using the LA-CCVD method without laser irradiation and with laser irradiation at different wavelengths.

Figure 6. Influence of the laser wavelength: (a) diamond deposition rate and (b) diamond quality factor (*Q*) as a function of laser wavelength.

Figure 7. Influence of the laser power density: (a) optical images of the acetylene-ethylene-oxygen flames without laser irradiation and with laser irradiation at different laser power densities, and (b) absorber laser power (left) and absorption coefficient (right) with respect to incident laser power densities, laser wavelength: 10.532 μm.

Figure 8. Influence of the laser power density: SEM micrographs diamond films deposited using the LA-CCVD method with laser irradiation at different power densities.

Figure 9. Influence of the laser power density: diamond film thickness (left) and deposition rate (right) as the functions of laser power density.

Figure 10. SEM micrographs of the diamond films and particles. (a-d) diamond films deposited without laser (a), with laser irradiation at 10.22 μm (b), 10.333 μm (c), and 10.532 (d). (e) and (f) single-crystal diamond grown with laser irradiation at 10.22 μm.

Figure 11. Mass spectrometry of $C_2H_2/C_2H_4/O_2$ flames. Relative concentrations of (a) C_xH_y (x = 1 and 2, y = 0 ~ 5) and (b) C_xH_yO (x = 1 and 2, y = 1 ~ 5) ions.

Figure 12. Absorption spectrum of the CO_2 laser power by NH_3 gas as a function of wavelength.

Figure 13. SEM micrographs of diamond films deposited using (a) NH_3-free flame without laser excitation, (b) NH_3-added flame without laser excitation, and (c - f) NH_3-added flame with laser excitation at 10.591, 10.719, 10.35 and 9.219 μm, respectively.

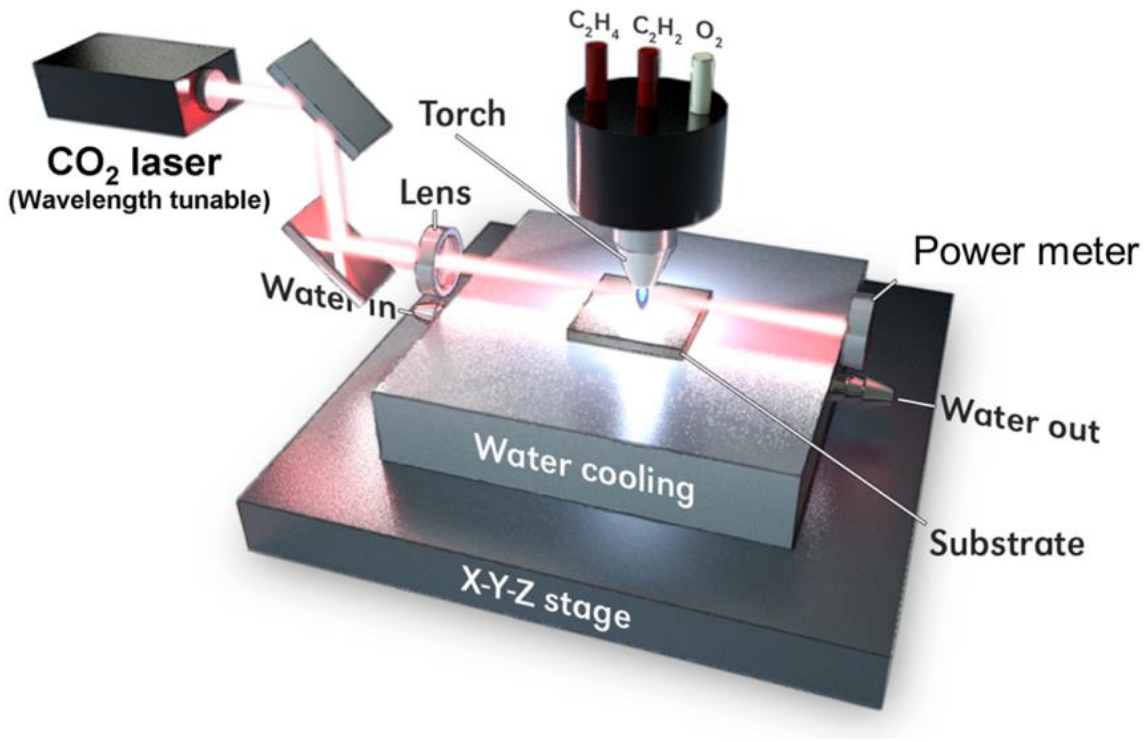
C_2H_4 C_2H_2 O_2
Torch
CO_2 laser
(Wavelength tunable)
Lens
Power meter
Water out
Water cooling
Substrate
X-Y-Z stage

Figure 1

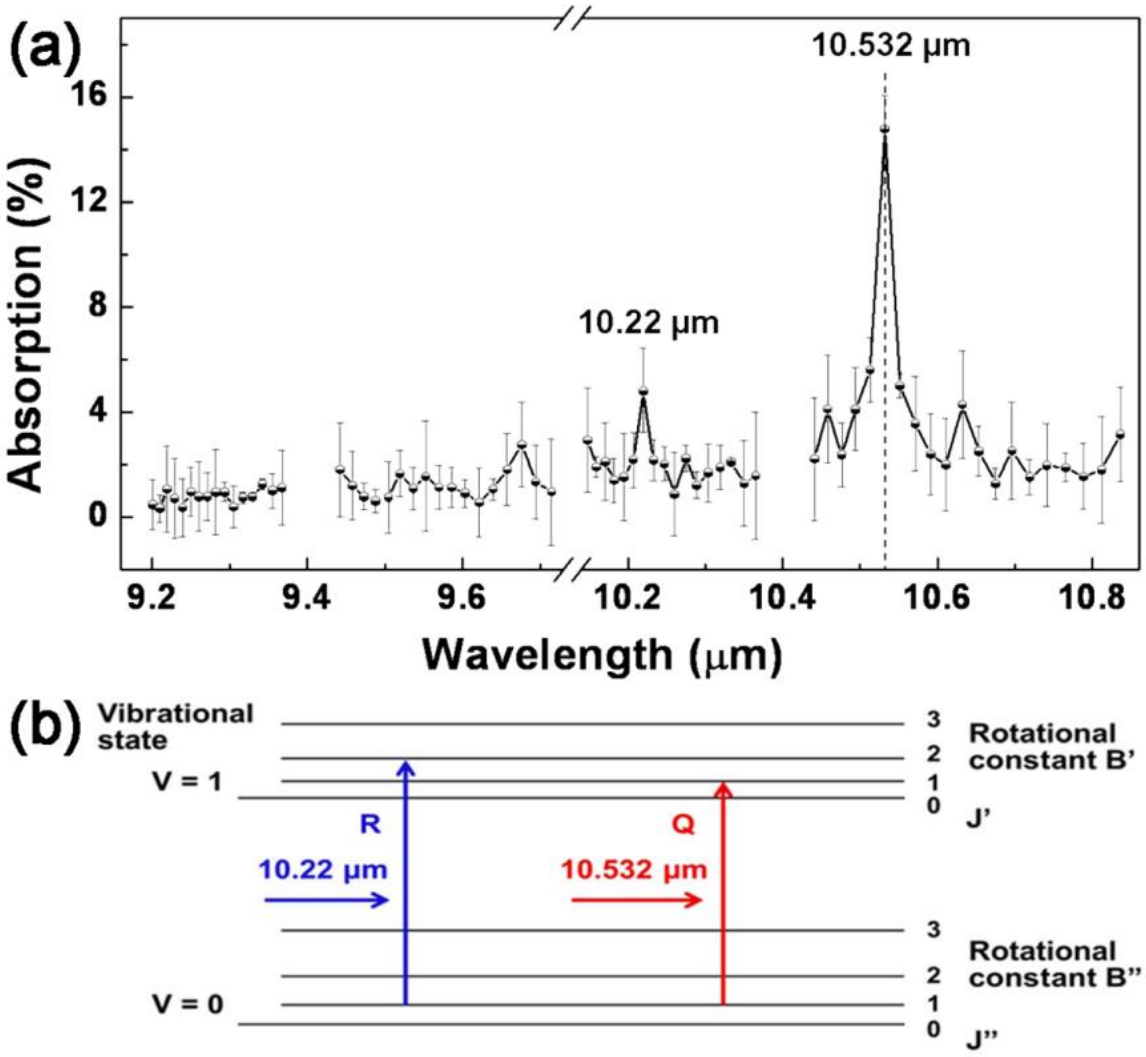
(a)
10.532 μm
10.22 μm
Absorption (%)
16
12
8
4
0
9.2
9.4
9.6
10.2
10.4
10.6
10.8
Wavelength (μm)
(b)
Vibrational state
V = 1
V = 0
R
Q
10.22 μm
10.532 μm
3
2
1
0
Rotational constant B'
J'
Rotational constant B"
J"

Figure 2

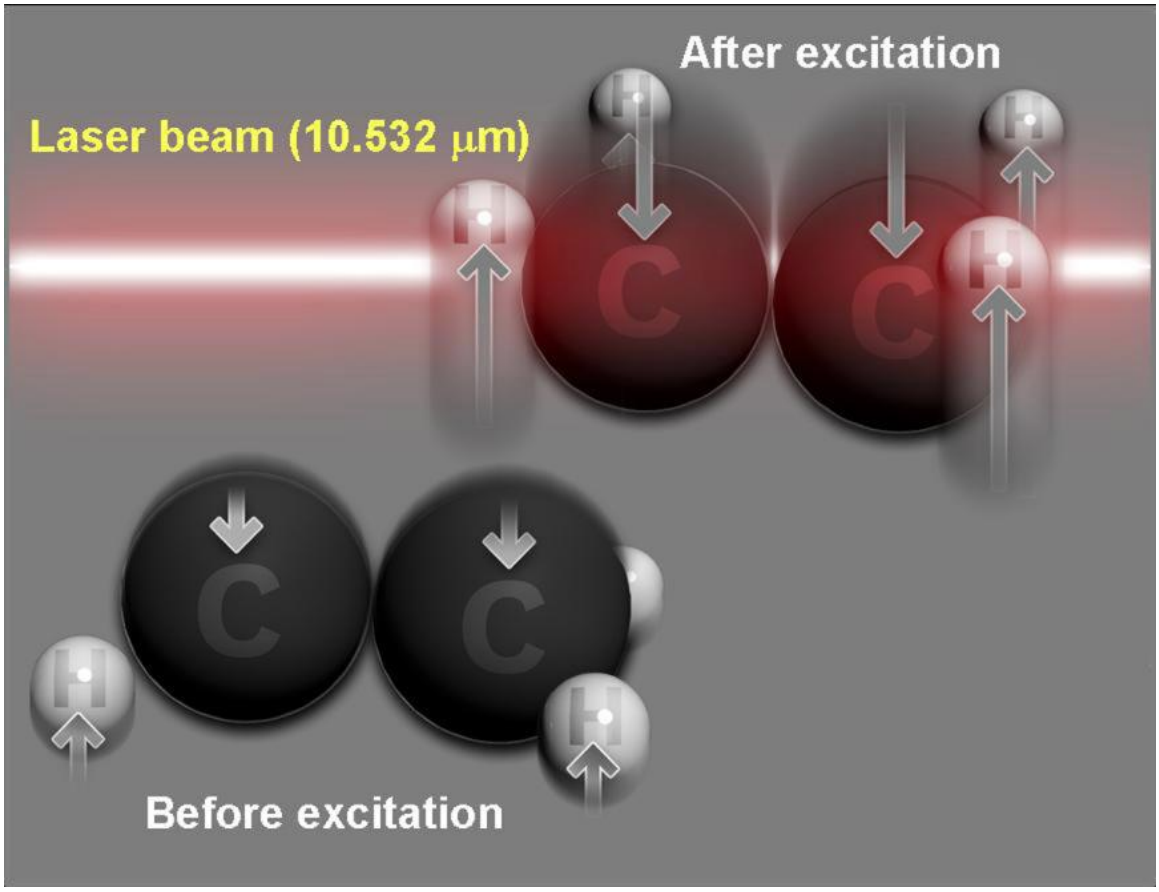
After excitation
Laser beam (10.532 μm)
C
C
C
C
Before excitation

Figure 3

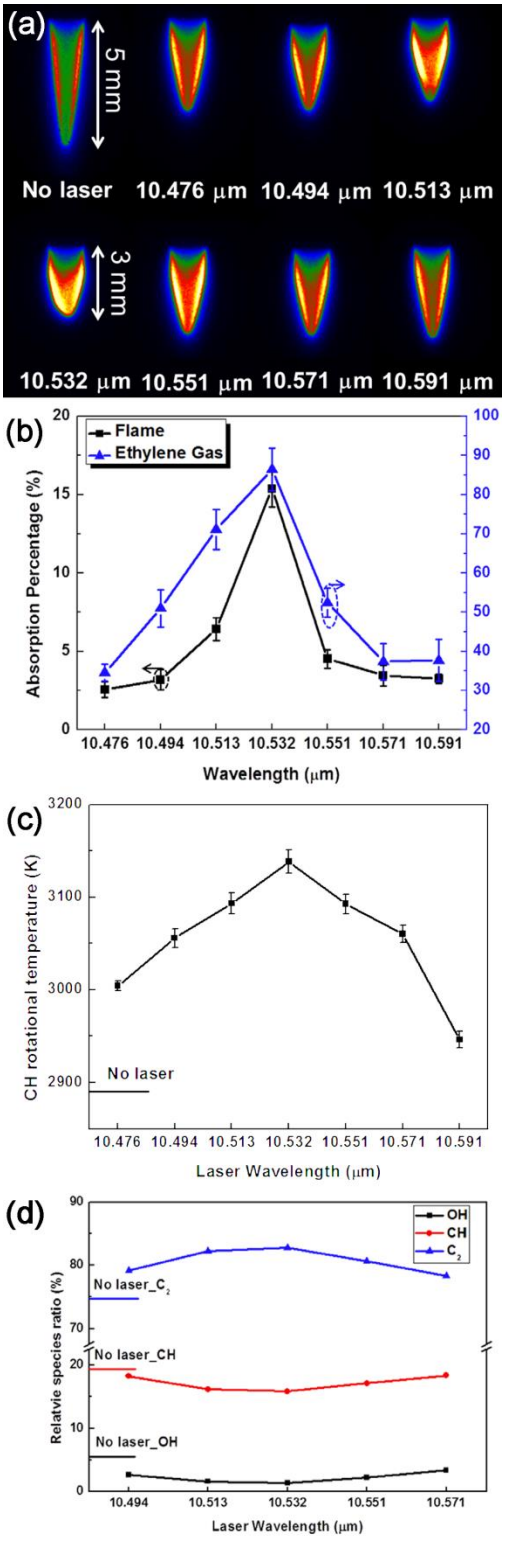
(a)
5 mm
No laser
10.476 μm
10.494 μm
10.513 μm
3 mm
10.532 μm
10.551 μm
10.571 μm
10.591 μm
(b)
Flame
Ethylene Gas
Absorption Percentage (%)
Wavelength (μm)
(c)
CH rotational temperature (K)
No laser
Laser Wavelength (μm)
(d)
OH
CH
C2
No laser_C2
No laser_CH
No laser_OH
Relatvie species ratio (%)
Laser Wavelength (μm)

Figure 4

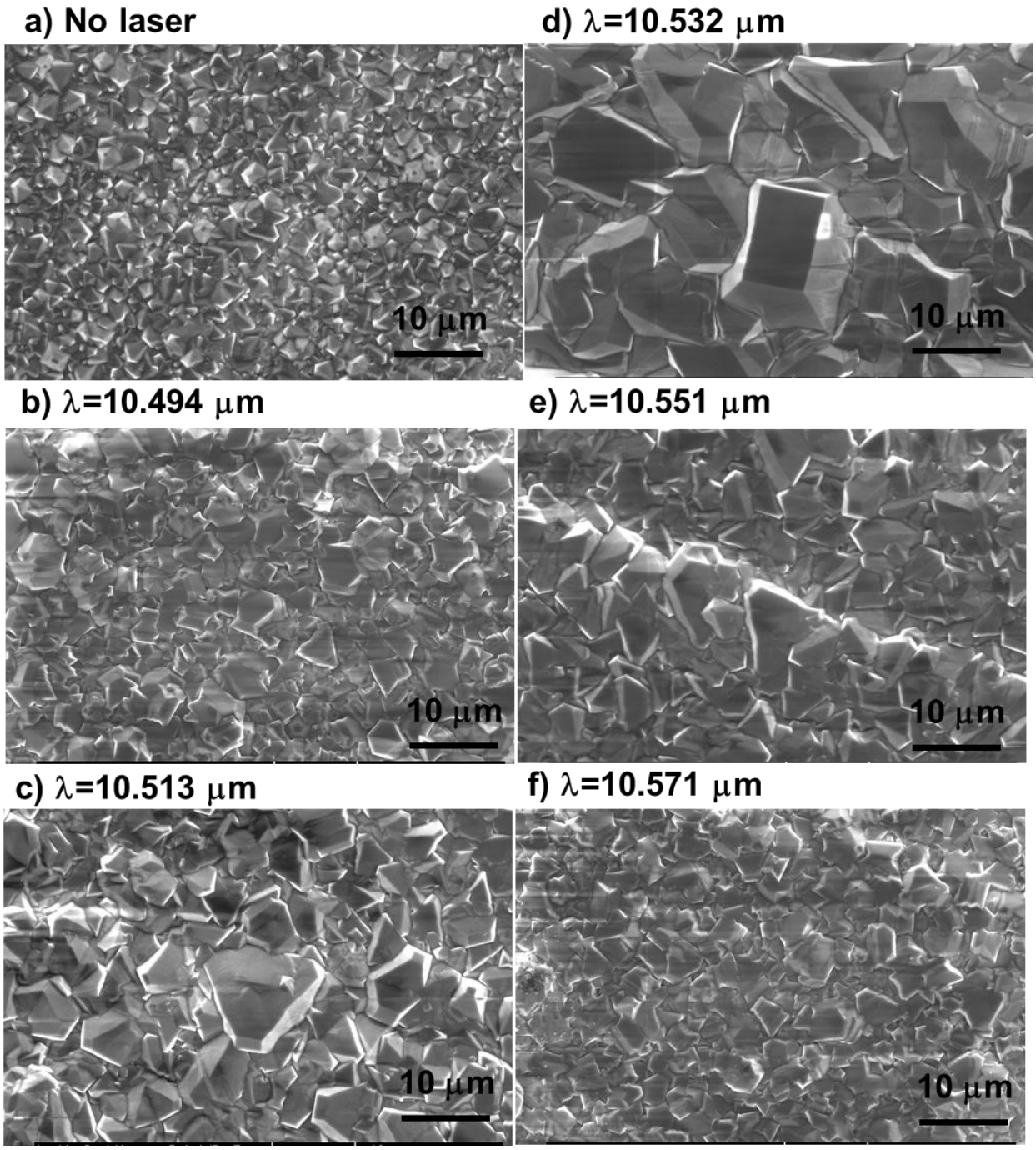
a) No laser
d) λ=10.532 μm
10 μm
10 μm
b) λ=10.494 μm
e) λ=10.551 μm
10 μm
10 μm
c) λ=10.513 μm
f) λ=10.571 μm
10 μm
10 μm

Figure 5

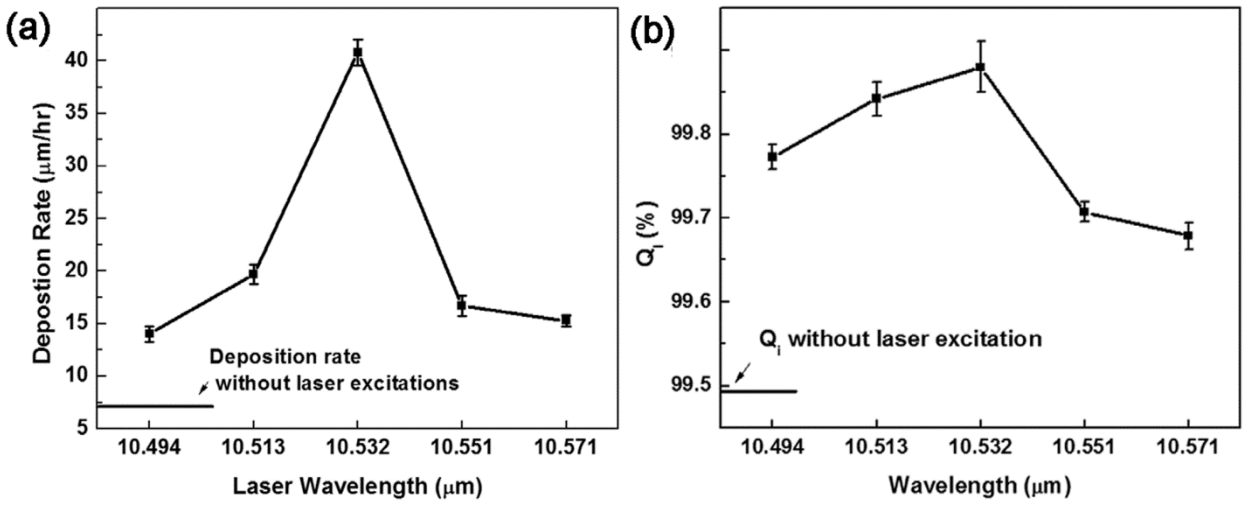
(a)
Depostion Rate (μm/hr)
40
35
30
25
20
15
10
5
Deposition rate
without laser excitations
10.494
10.513
10.532
10.551
10.571
Laser Wavelength (μm)
(b)
Q_i (%)
99.8
99.7
99.6
99.5
Q_i without laser excitation
10.494
10.513
10.532
10.551
10.571
Wavelength (μm)

Figure 6

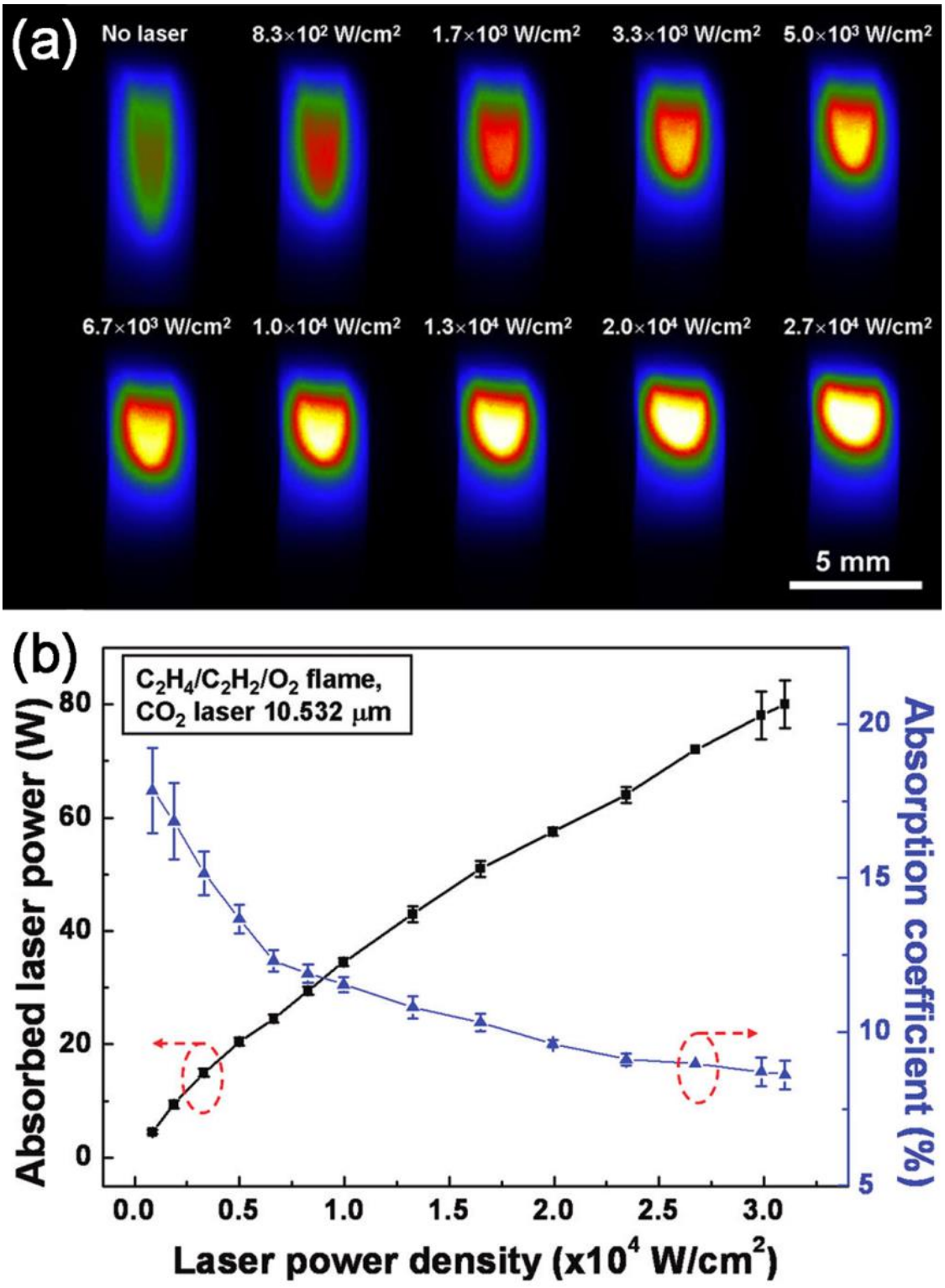
(a)
No laser
8.3×10² W/cm²
1.7×10³ W/cm²
3.3×10³ W/cm²
5.0×10³ W/cm²
6.7×10³ W/cm²
1.0×10⁴ W/cm²
1.3×10⁴ W/cm²
2.0×10⁴ W/cm²
2.7×10⁴ W/cm²
5 mm
(b)
C2H4/C2H2/O2 flame,
CO2 laser 10.532 μm
Absorbed laser power (W)
Absorption coefficient (%)
Laser power density (x10⁴ W/cm²)
0
20
40
60
80
5
10
15
20
0.0
0.5
1.0
1.5
2.0
2.5
3.0

Figure 7

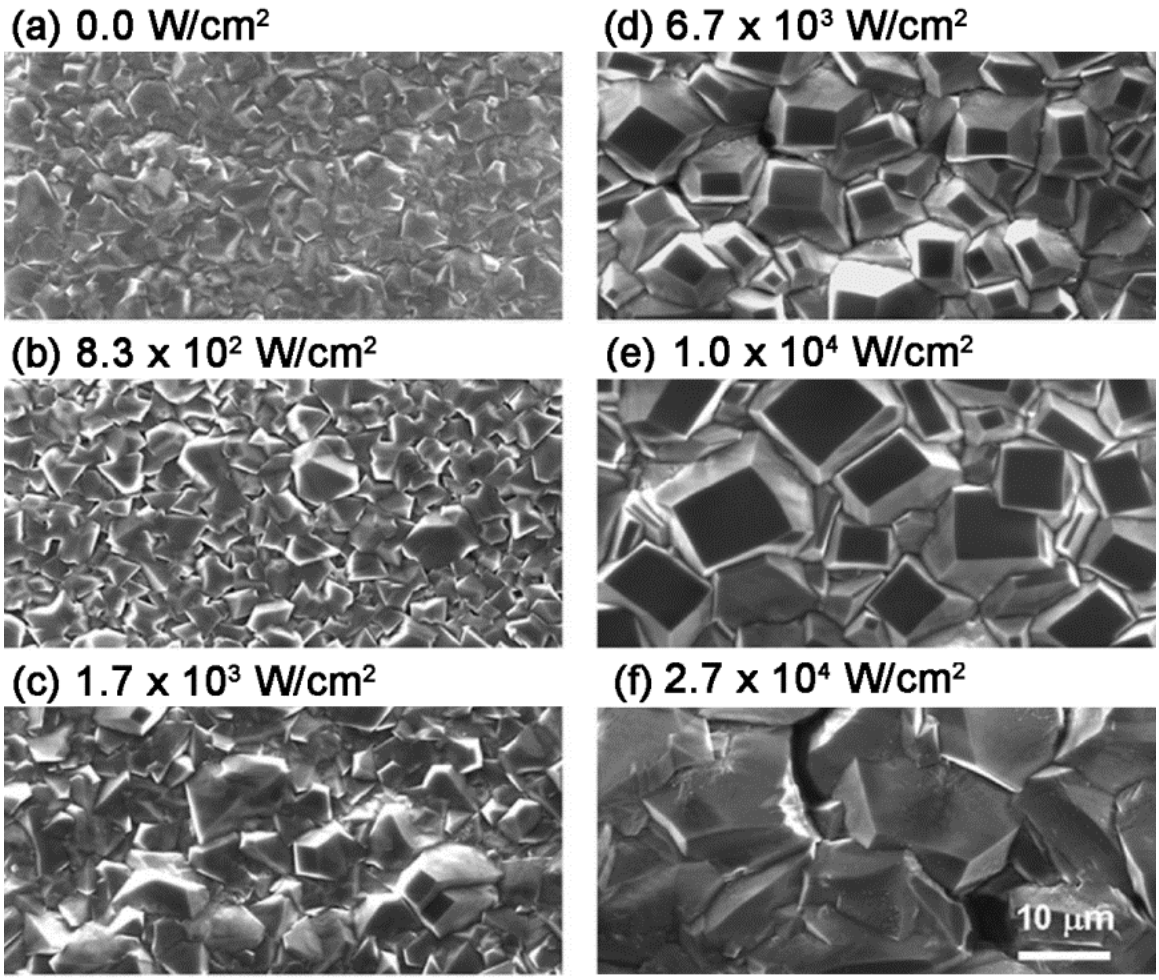
(a) 0.0 W/cm²
(d) 6.7 x 10³ W/cm²
(b) 8.3 x 10² W/cm²
(e) 1.0 x 10⁴ W/cm²
(c) 1.7 x 10³ W/cm²
(f) 2.7 x 10⁴ W/cm²
10 μm

Figure 8

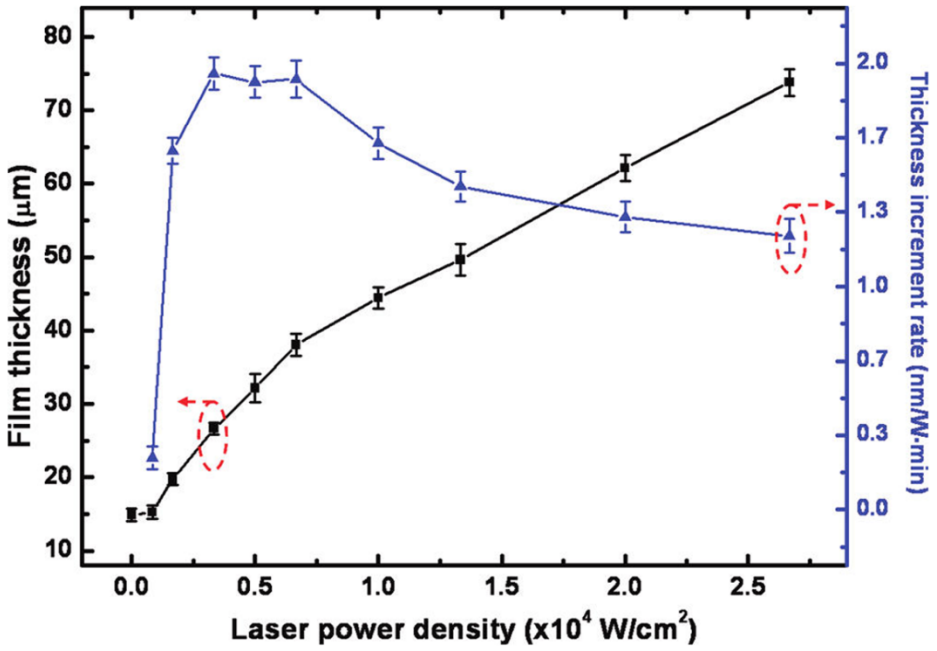
Film thickness (μm)
Thickness increment rate (nm/W·min)
Laser power density (x10^4 W/cm^2)
80
70
60
50
40
30
20
10
2.0
1.7
1.3
1.0
0.7
0.3
0.0
0.0
0.5
1.0
1.5
2.0
2.5

Figure 9

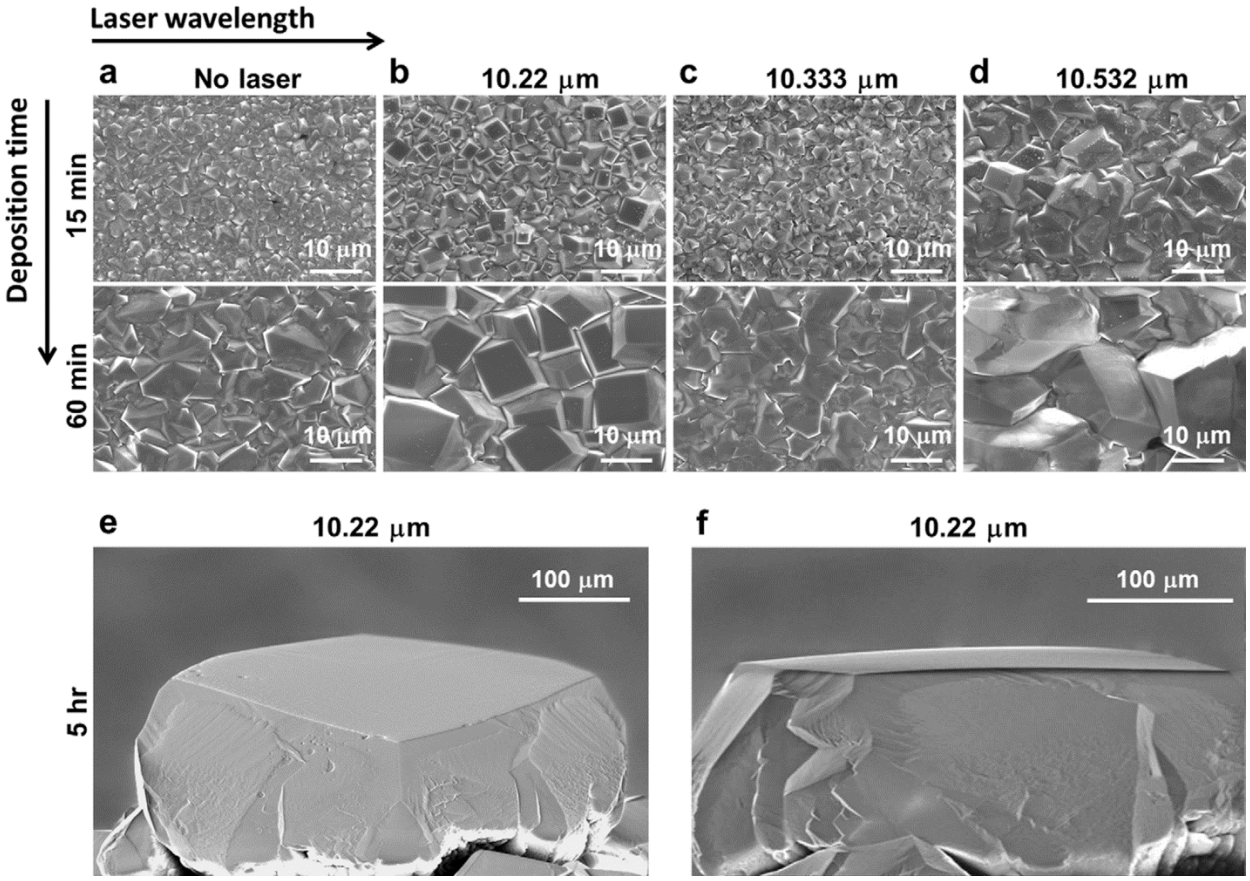
Laser wavelength
a
No laser
b
10.22 μm
c
10.333 μm
d
10.532 μm
Deposition time
15 min
60 min
10 μm
e
10.22 μm
f
10.22 μm
5 hr
100 μm

Figure 10

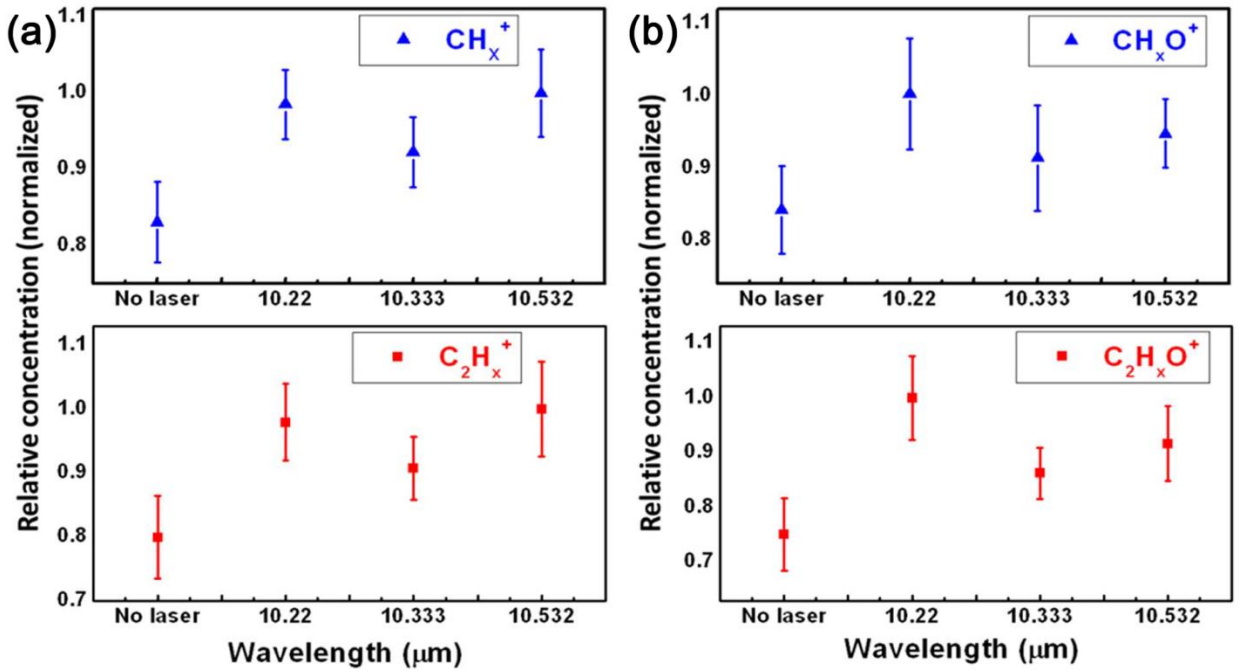
(a)
(b)
Relative concentration (normalized)
Wavelength (μm)
No laser
10.22
10.333
10.532
CH$_x^+$
C$_2$H$_x^+$
CH$_x$O$^+$
C$_2$H$_x$O$^+$

Figure 11

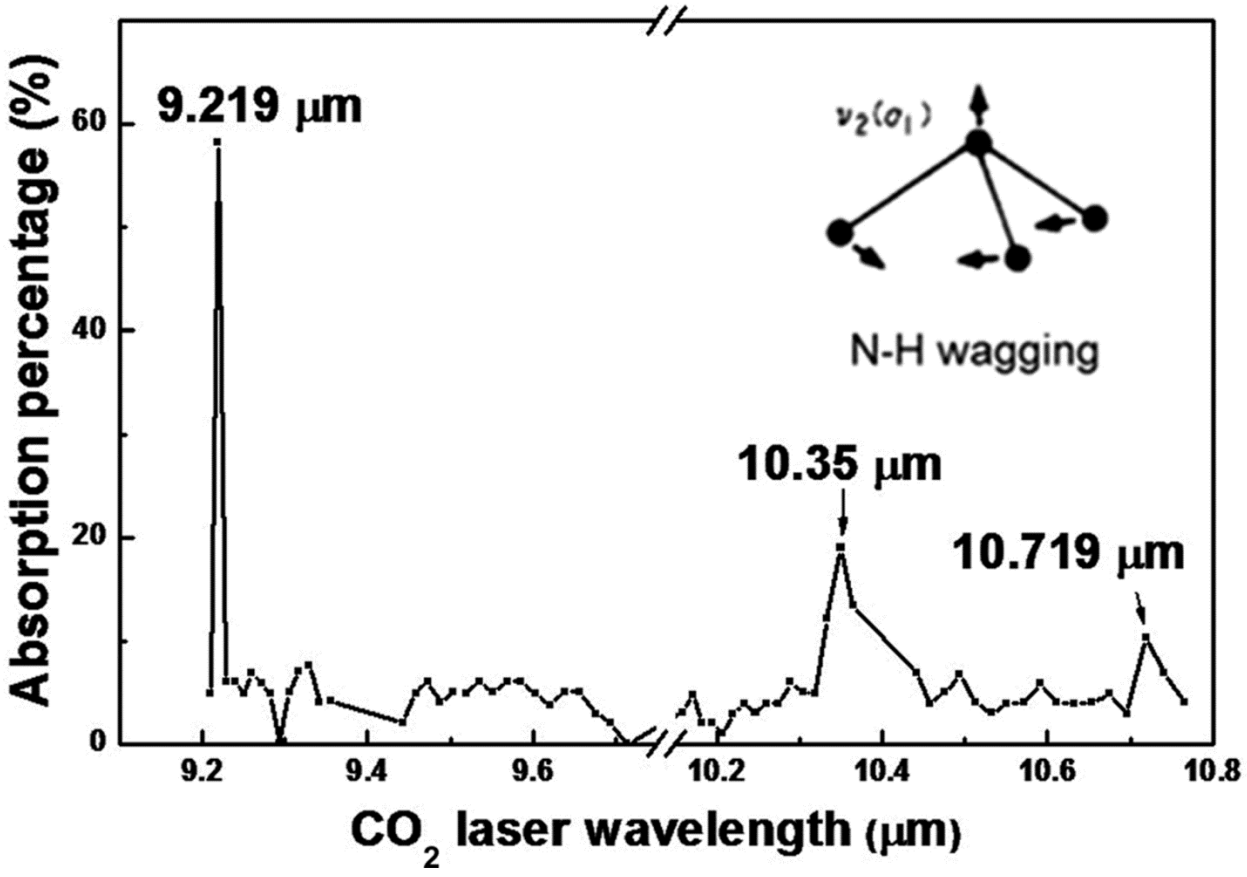
9.219 μm
10.35 μm
10.719 μm
N-H wagging
Absorption percentage (%)
0
20
40
60
9.2
9.4
9.6
10.2
10.4
10.6
10.8
CO2 laser wavelength (μm)

Figure 12

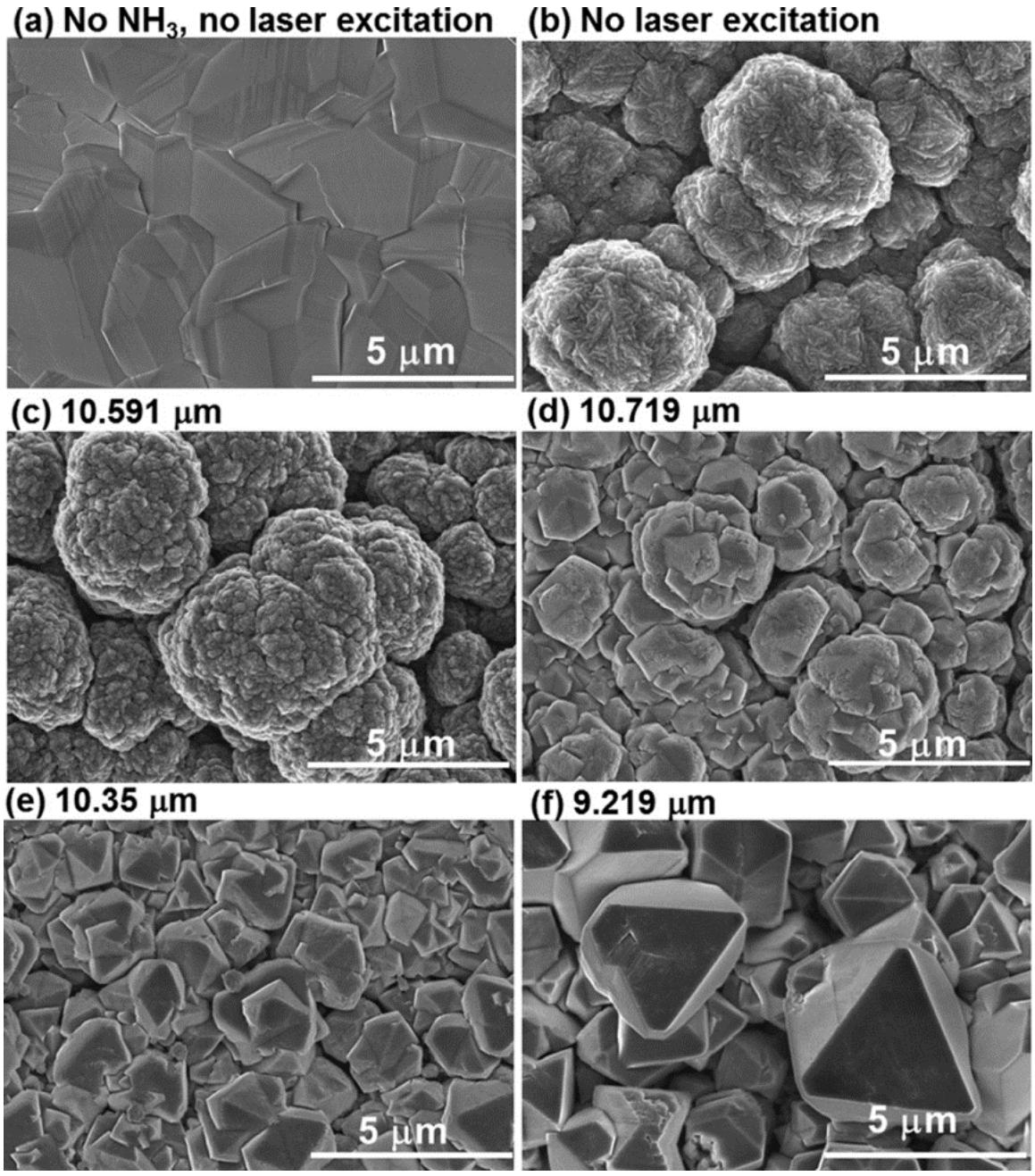
(a) No NH3, no laser excitation
(b) No laser excitation
(c) 10.591 μm
(d) 10.719 μm
(e) 10.35 μm
(f) 9.219 μm
5 μm

Figure 13